

Jet production in $\gamma\gamma$ collisions at LEP

Thorsten Wengler, CERN

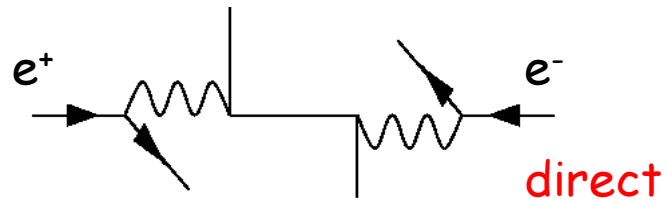
- ⇒ (Di-) Jet production mechanisms in $\gamma\gamma$ – collisions
- ⇒ Single jet inclusive
- ⇒ Di-jet inclusive
- ⇒ Jet structure in di-jet events



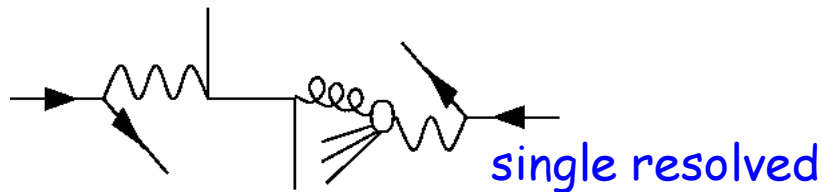
(Di-) jet production mechanisms in $\gamma\gamma$ -collisions

$\gamma\gamma$ collisions @ LEP

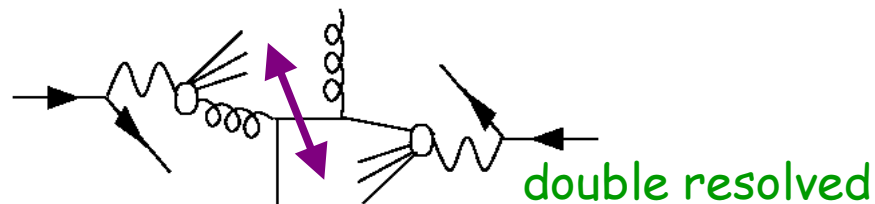
\Rightarrow compared to ep collisions @ HERA



\Rightarrow does not exist
(proton is always "resolved" here)



\Rightarrow direct



\Rightarrow resolved

multiple parton interactions (MIA)?

Only photons with virtuality $Q^2 \approx 0$ are considered
 \Rightarrow electrons are not tagged ("untagged $\gamma\gamma$ events")

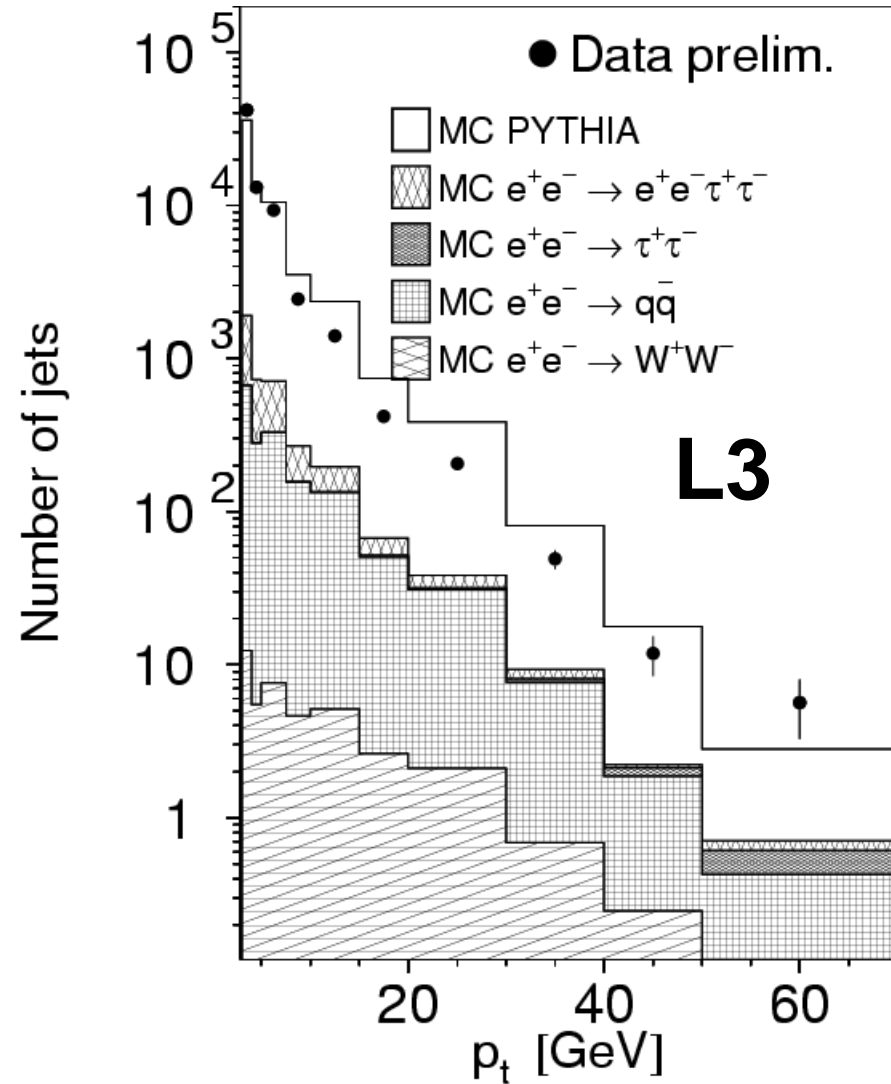
Single jets inclusive (L3)

Data sample

- $\sqrt{s} = 189\text{-}208 \text{ GeV}$
- $\mathcal{L} = 560 \text{ pb}^{-1}$

Event / Jet selection

- Standard $\gamma\gamma$ -selection
 - Hadronic final state with > 6 tracks/clusters
 - Detected Energy $< 0.4 \sqrt{s}$
 - No tagged electrons in forward calorimeters
- ⇒ 1% background left (10 % at high p_T)
- Inclusive k_{\perp} ($R_0=1.0$) with $p_T > 3 \text{ GeV}$, $|\eta| < 1$



Single jet inclusive cross-section

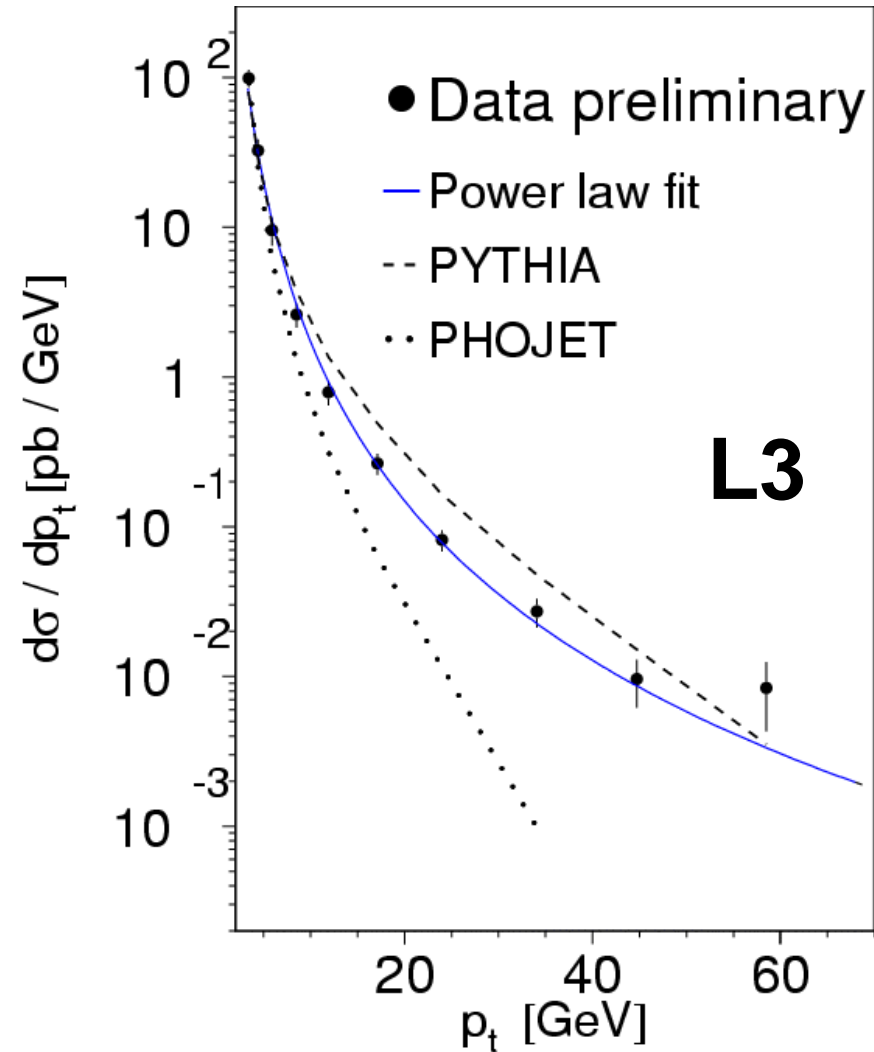
The data can be described
by a power law

$$A p_T^{-B}$$

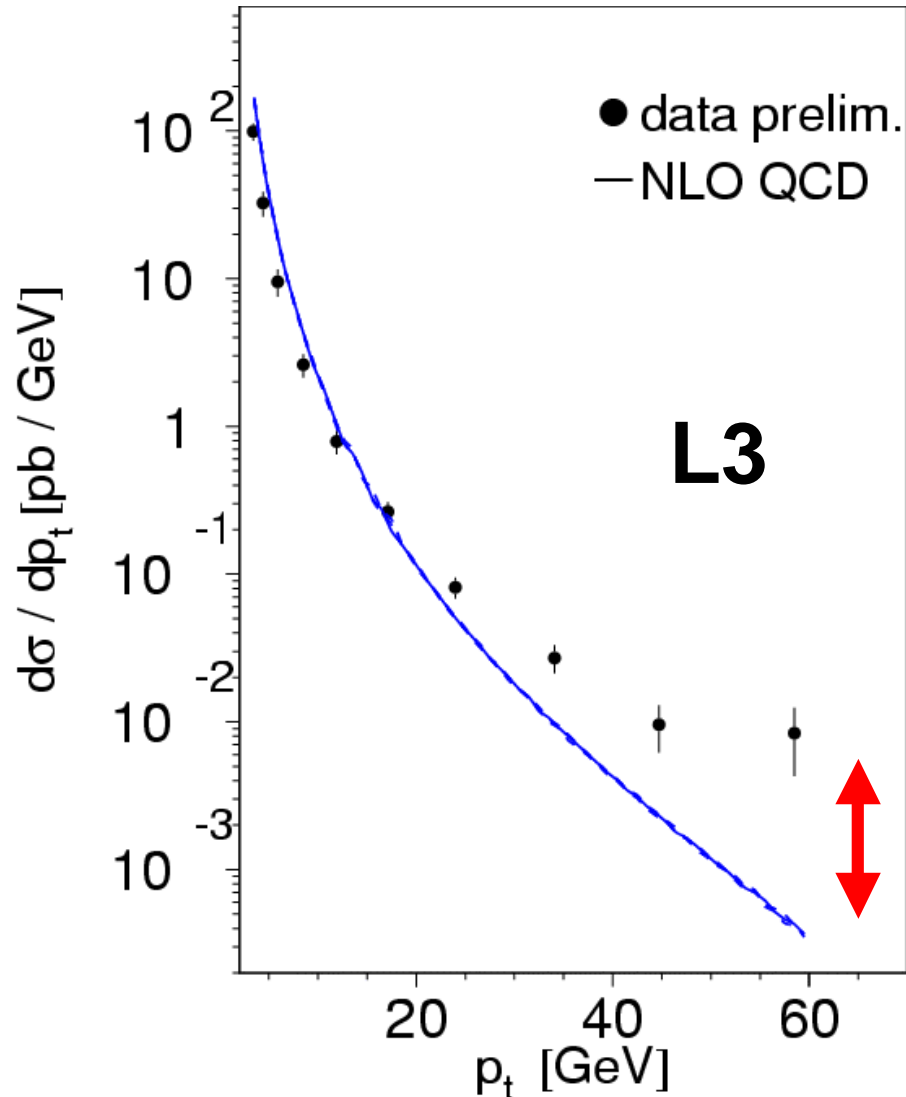
A fit yields $B \sim 3.5$

PHOJET 1.05 way too low
at high p_T

PYTHIA 5.722 is closer,
but too large and also
no good description at high p_T



Single jet inclusive cross-section cont.



NLO: L. Bertora, S. Frixione

The shape is well described below ~ 15 GeV by NLO QCD

NLO is (much) lower than the data at high p_t

This is consistent with the observations in charged and neutral hadron production by L3

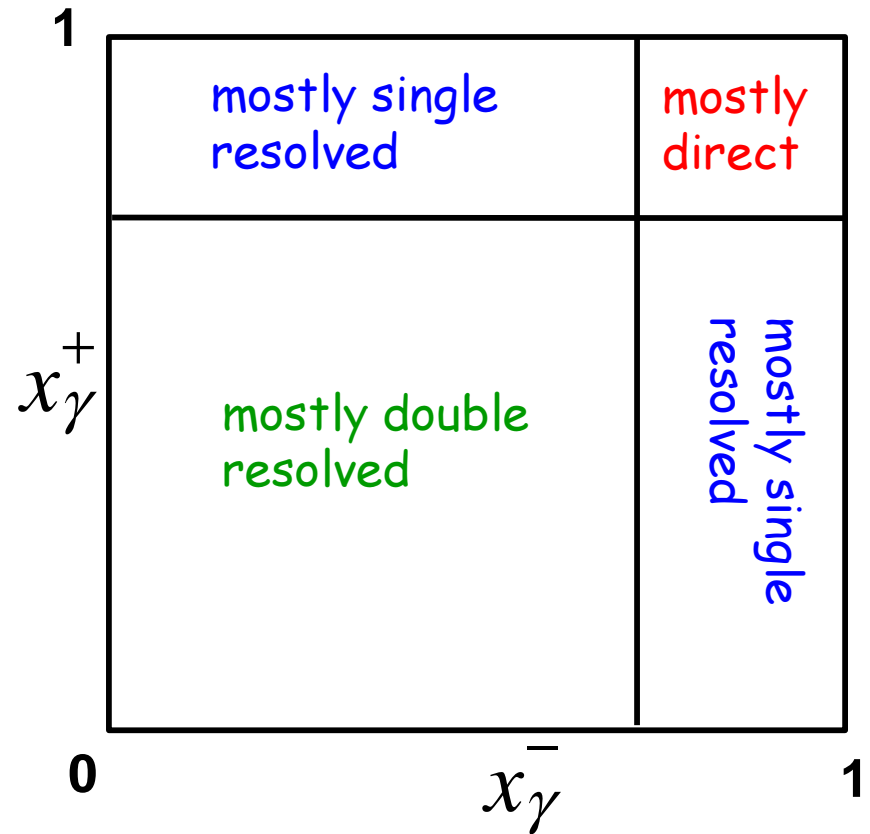
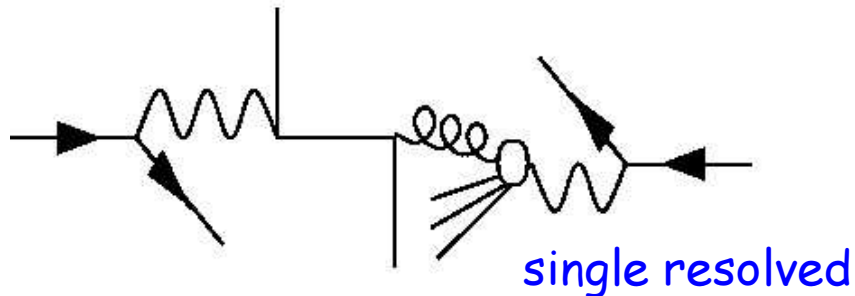
Di-jet: more access to the "inside"

Estimate of fraction of photon momentum entering hard collision

$$x_\gamma^\pm = \frac{\sum_{jet1,2} E^\pm p_Z}{\sum_{hadrons} E^\pm p_Z}$$

$$x_\gamma \cong 1$$

$$x_\gamma < 1$$



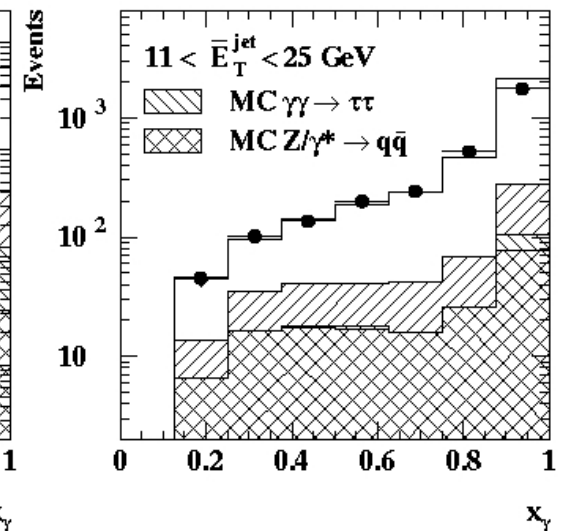
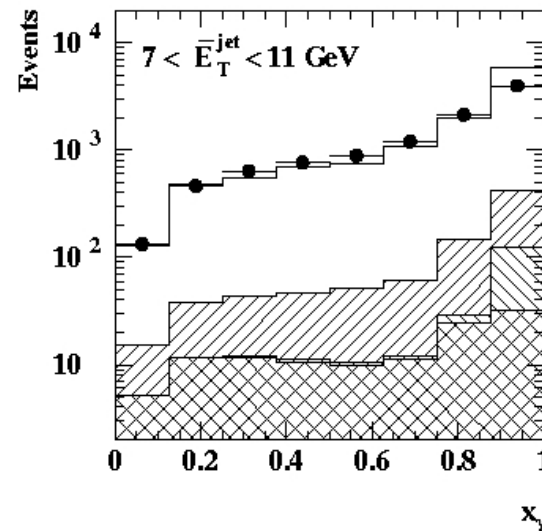
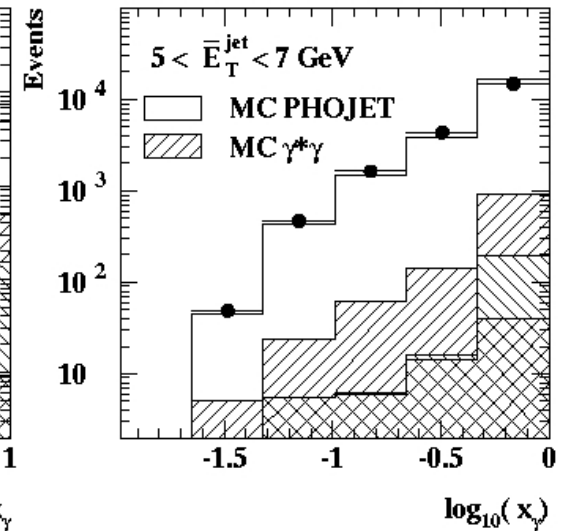
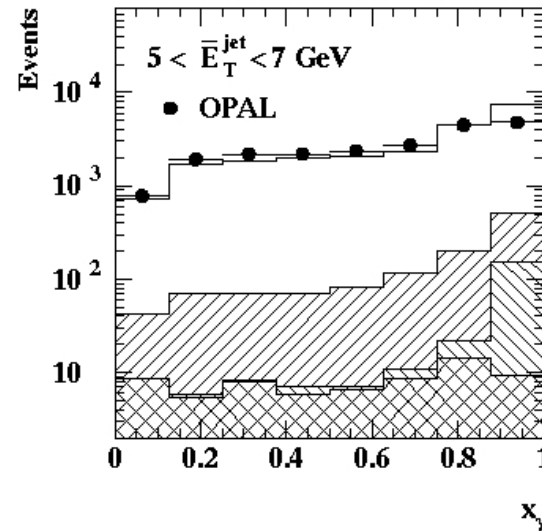
Data selection and background (OPAL)

Data sample

- $\sqrt{s} = 189\text{-}209 \text{ GeV}$
- $\mathcal{L} = 593 \text{ pb}^{-1}$

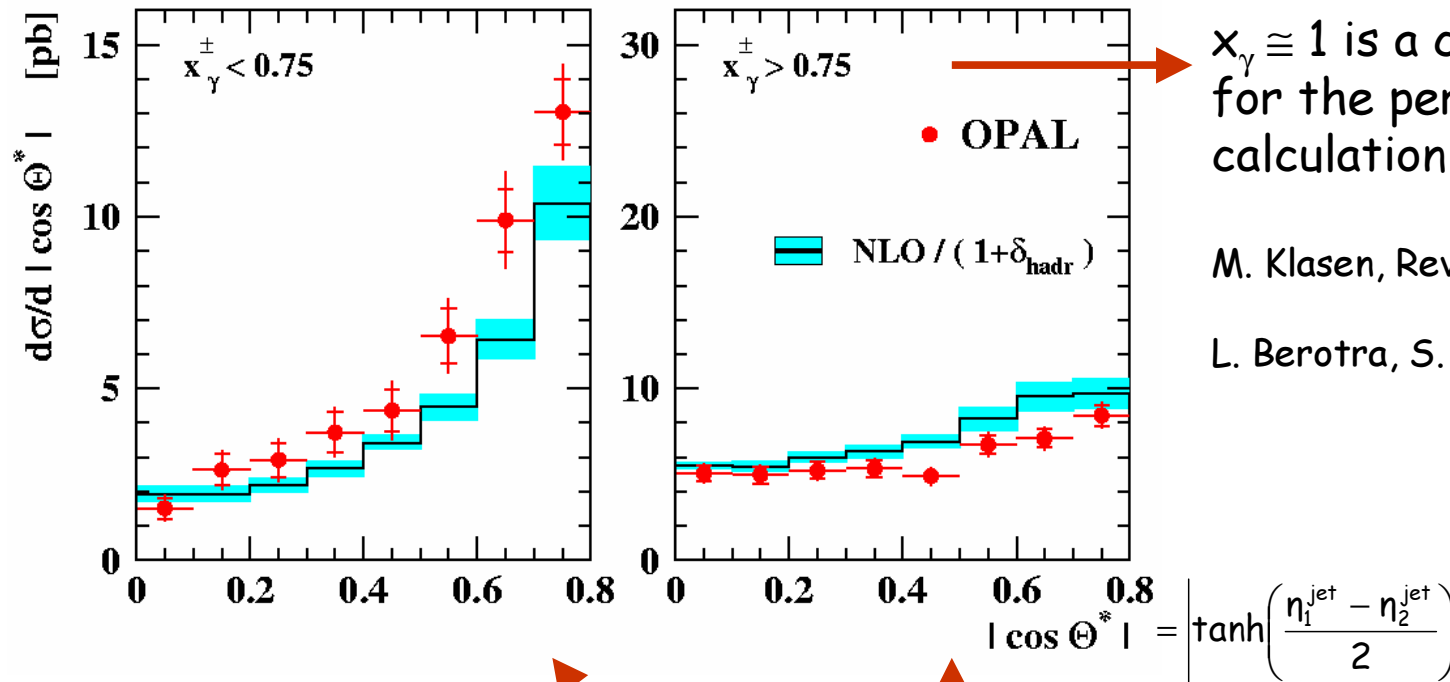
Event / Jet selection

- Standard $\gamma\gamma$ -selection
 \Rightarrow 5% background left
 (10-15% at high E_T)
- Inclusive k_{\perp} ($R_0=1.0$) with
 mean $E_T > 5 \text{ GeV}$, $|\eta| < 2$,
 $|\Delta E_{T,1,2}| / \Sigma E_{T,1,2} < 0.25$
 for cross-sections
- k_{\perp} and cone ($\eta\phi$ -radius = 1.0)
 for jet structure comparisons



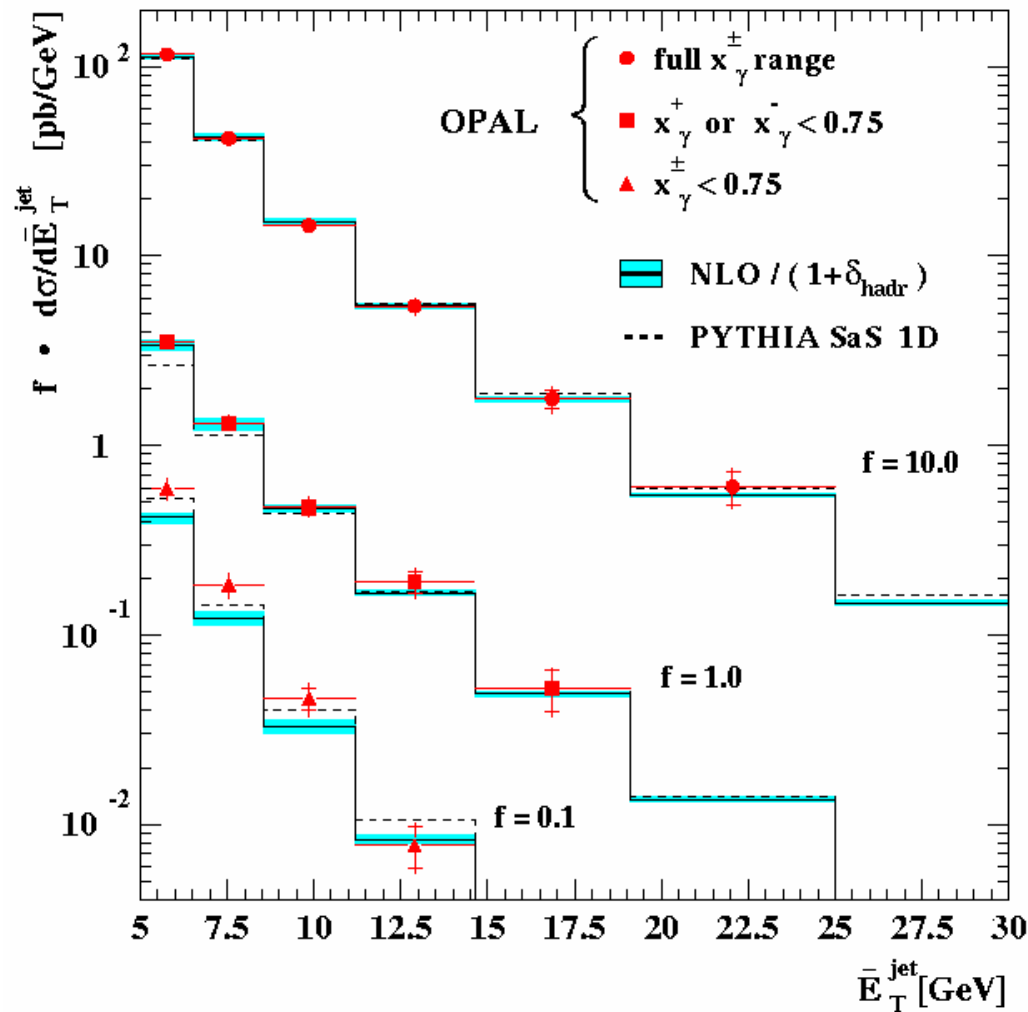
Di-jet angular distributions: quarks vs. gluons

NLO: Klasen et al.



Different shape for gluon and quark dominated sample

The di-jet cross-section vs. mean E_T^{jet}



Well described by NLO for
total sample and

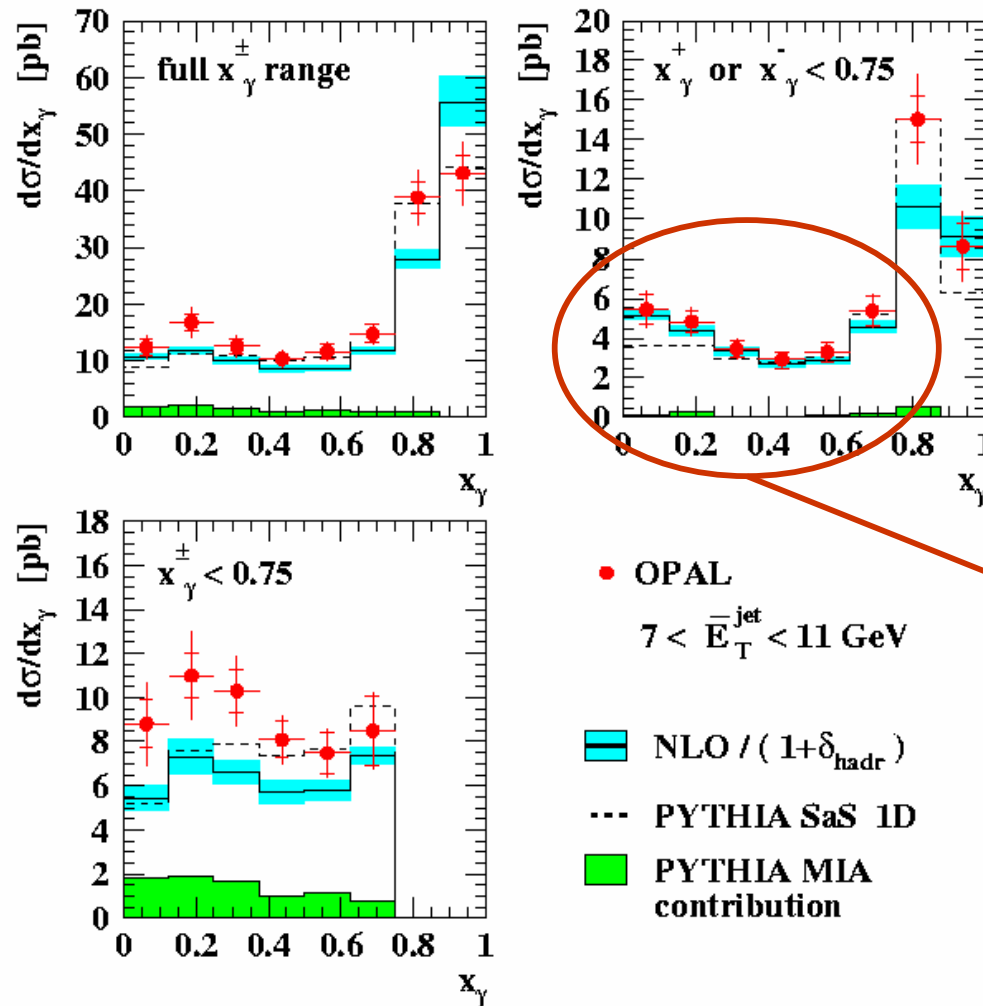
“single resolved enhanced”

But too low for

“double resolved enhanced”

Which might be due to ...

The di-jet cross-section vs. x_γ



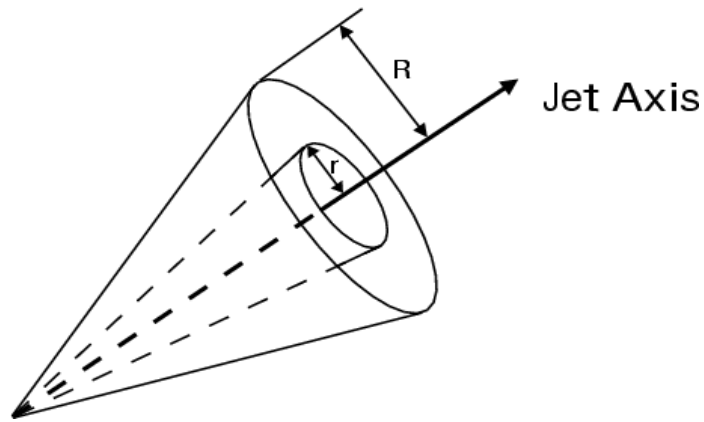
...MIA, which (PYTHIA says),
 are very small for single res.
 enhanced sample, as expected.



Small hadronisation
 corrections and no
 disturbance from MIA

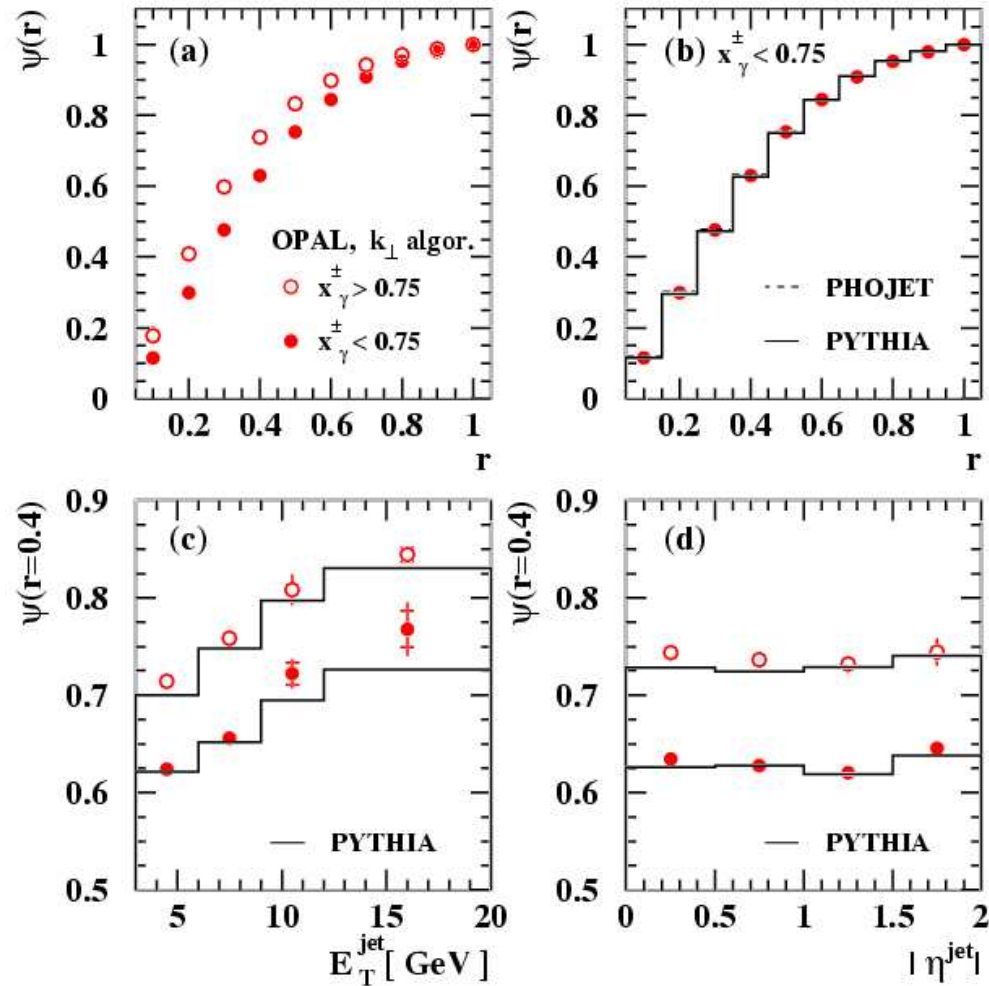
NLO should work here -
 and it does!

The internal structure of jets: quarks vs. gluons

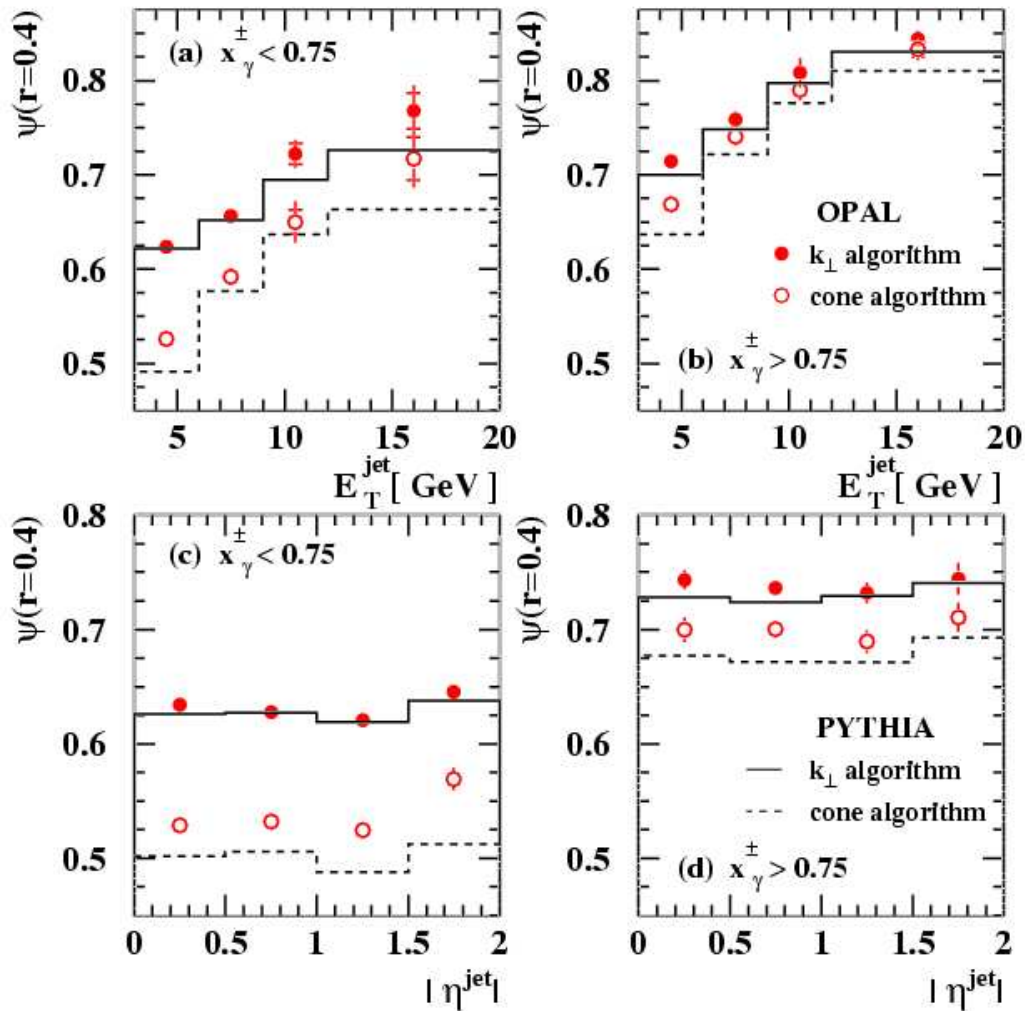


$$\psi(r) = \frac{1}{N_{\text{jets}}} \sum_{\text{jets}} \frac{E_T^{\text{jet}}(r)}{E_T^{\text{jet}}(R=r|_{1.0})}$$

$$r = \sqrt{(\Delta\eta)^2 + (\Delta\phi)^2}$$



The internal structure of jets cont.



Quark jets are more collimated than gluon jets, but both show the same dependence on E_T and η

k_\perp jets are more collimated than cone jets and are better described by the Monte Carlo

Conclusions

Single jet (L3) and Di-jet (OPAL) production has been studied in 2-photon collisions at LEP

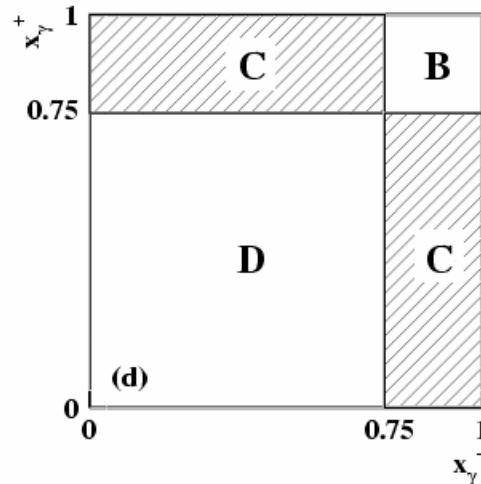
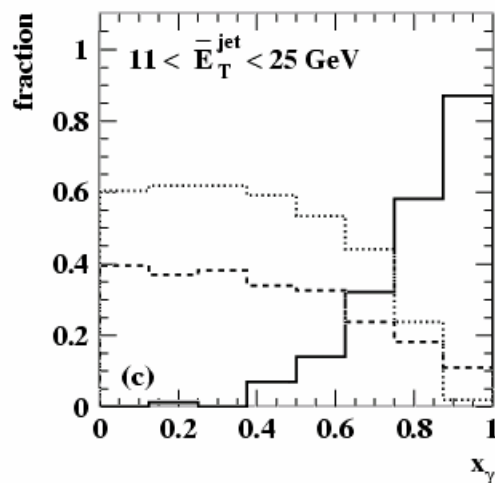
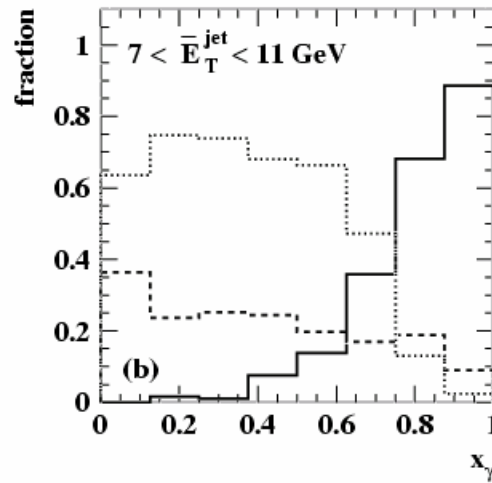
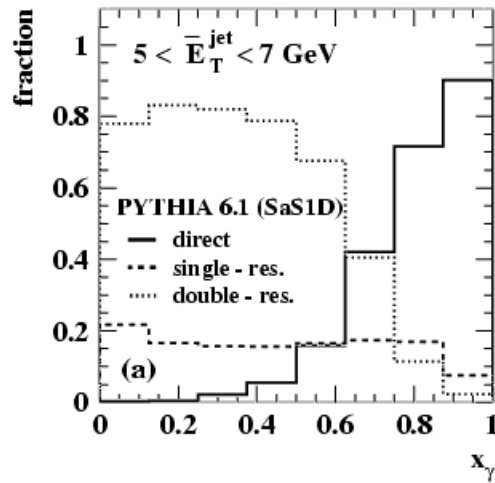
The single jet cross section is underestimated by NLO at high p_T (as seen in hadron production before)

Di-jet cross-section are measured in regions with small and regions with large expected contributions from MIA

NLO QCD agrees well with the di-jet data in regions where it is expected to be reliable.

Quark and gluon dominated sub-samples in di-jet events are studied and show the behavior expected from QCD for jet structure and angular distributions

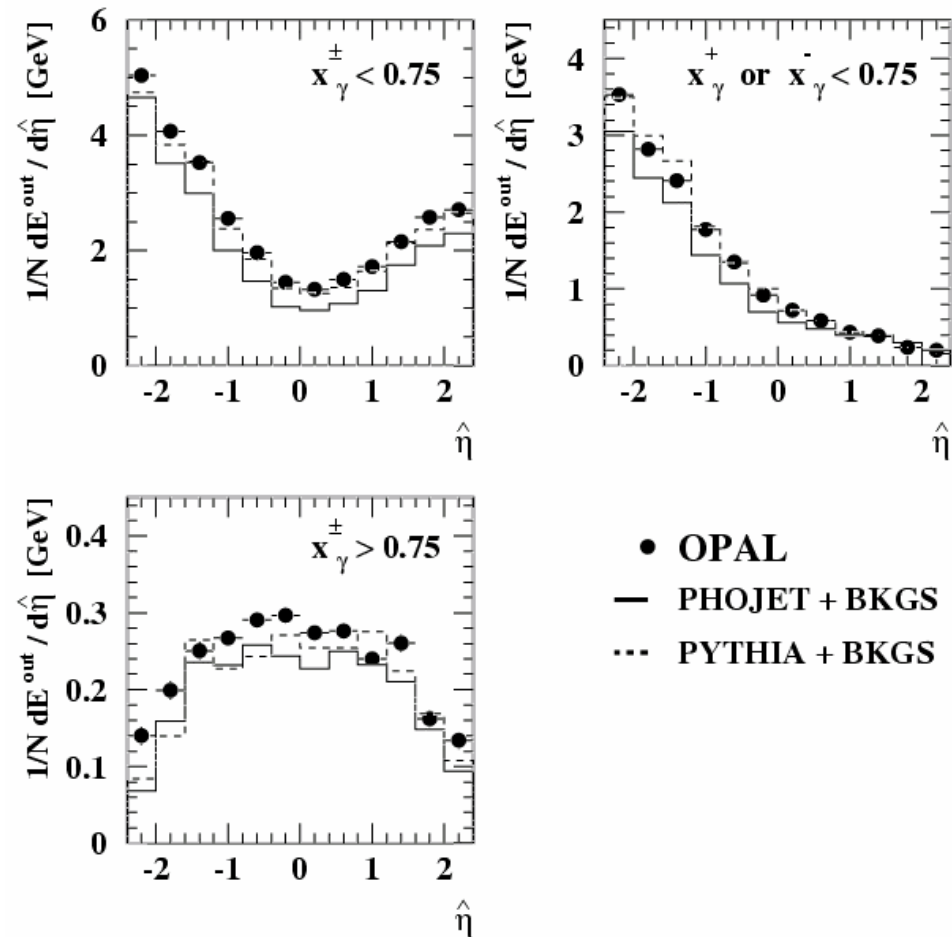
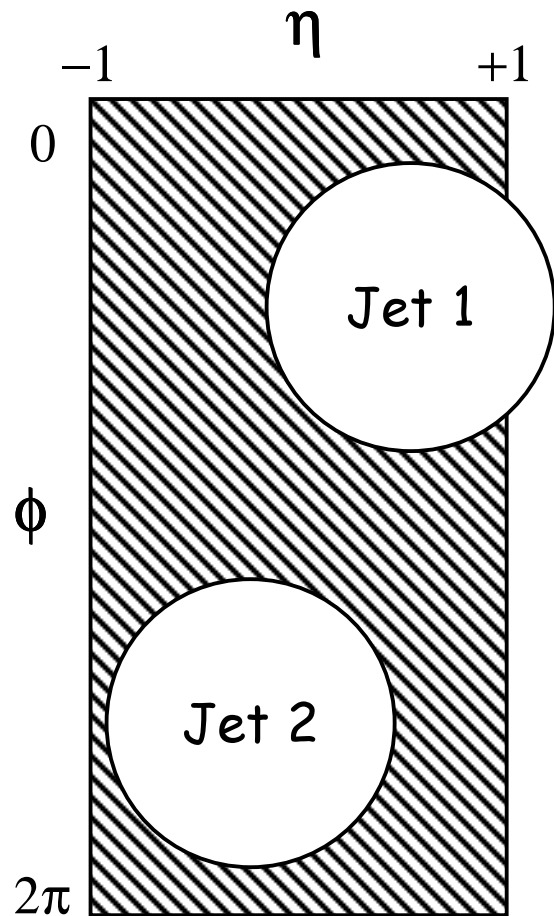
Resolved vs. direct event fractions (OPAL)



For higher jet energies
the fraction of
resolved events at low
 x_γ is still high

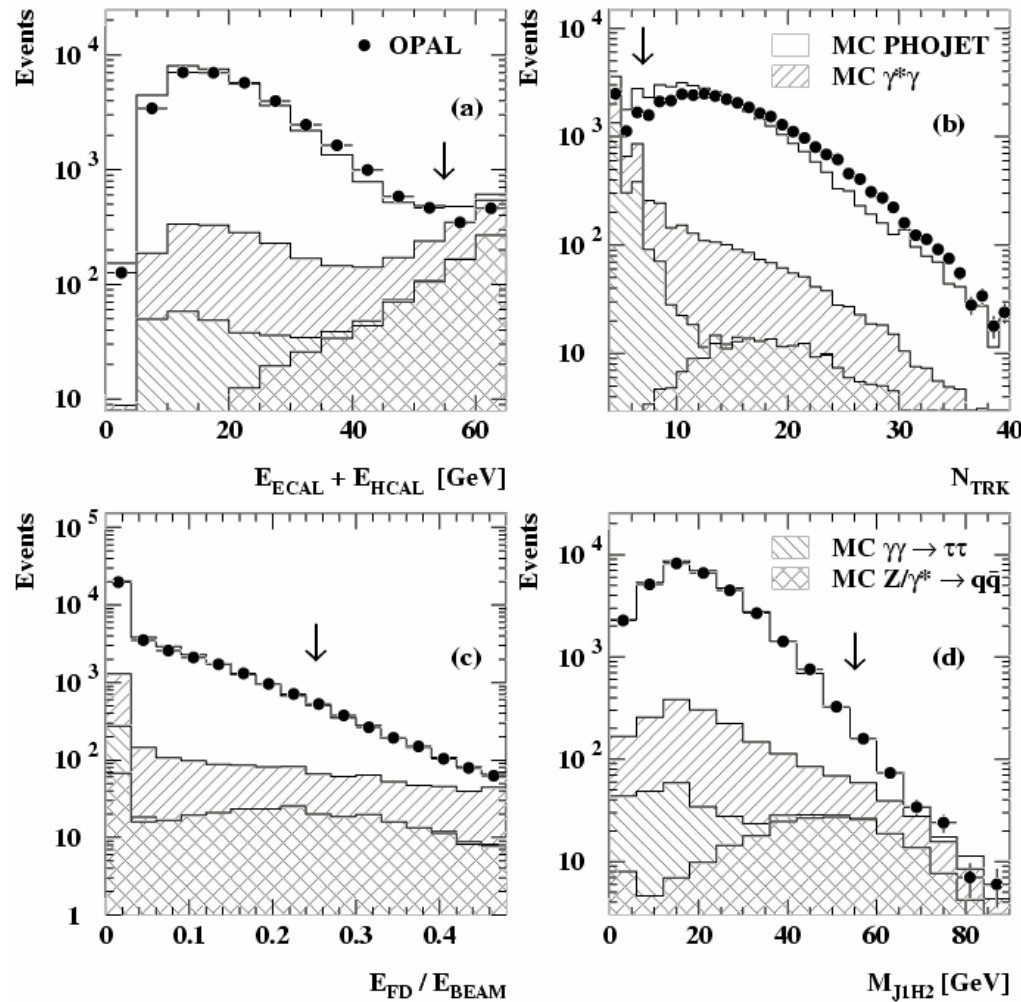
(but the cross-section
decreases)

Energy flow outside the two leading jets (OPAL)



Energy flow in shaded region vs. η ordered by x_γ (more resolved γ is left)

Selection of the $\gamma\gamma$ -sample (OPAL)



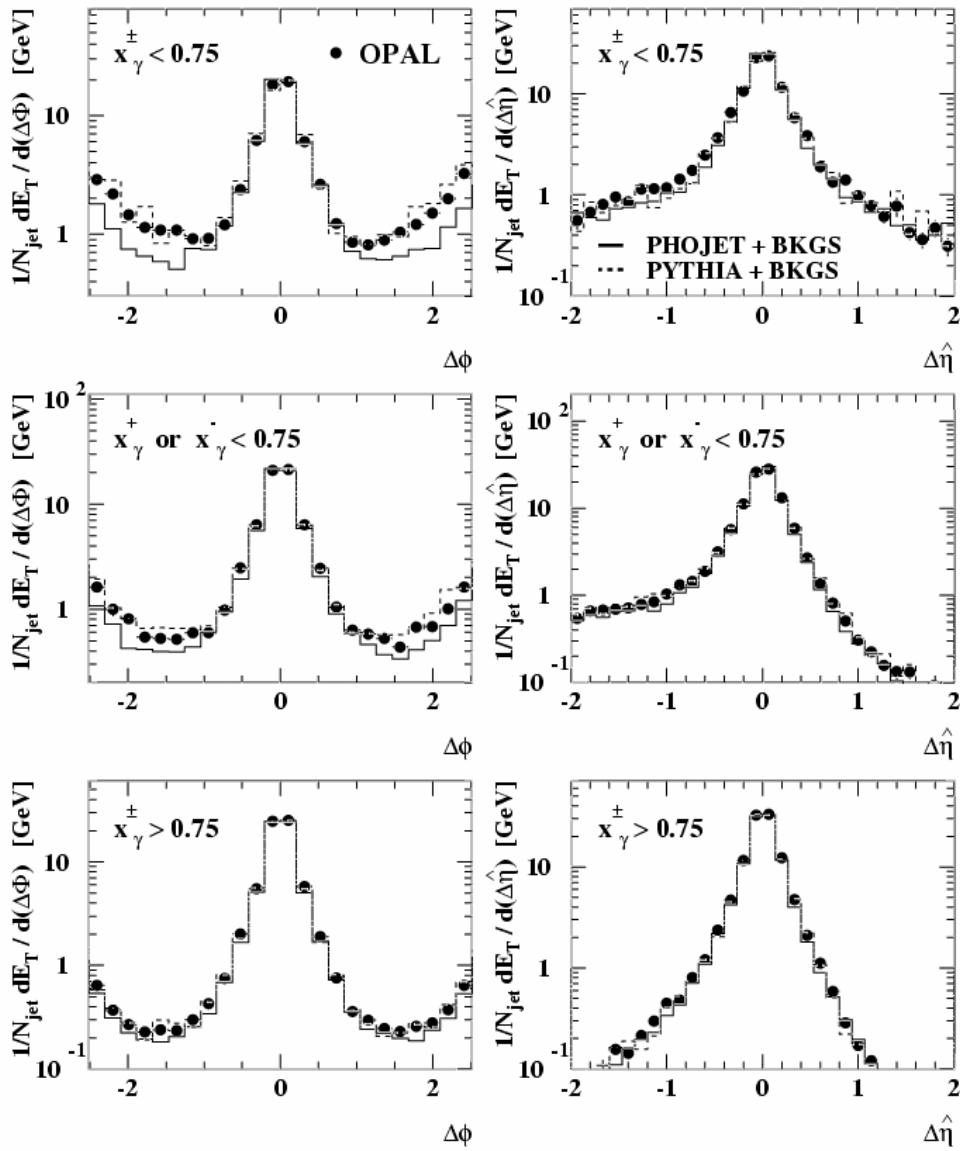
Standard $\gamma\gamma$ event selection:

- ΣE_{calo} & (Leading jet ,opposite hemisphere)_{inv.mass} < 55 GeV
- Number of tracks > 6
- Antitag in forward detectors
- Quality cuts on missing momentum, vertex position
- Total remaining background is about 5%

The arrows indicate the cut value

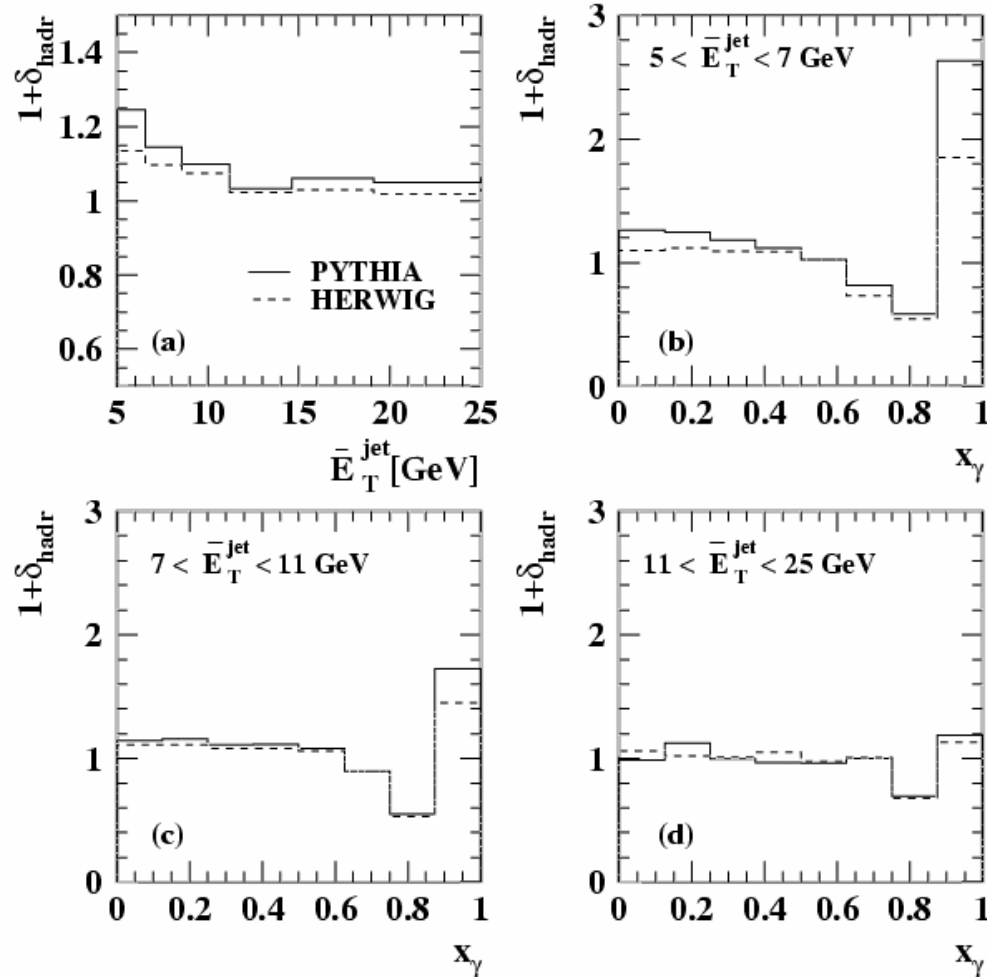
In each case all cuts are applied except on the quantity shown

Energy flow around jets (jet profiles) (OPAL)



Some discrepancy for PHOJET in region between jets, but well described by Monte Carlo in general

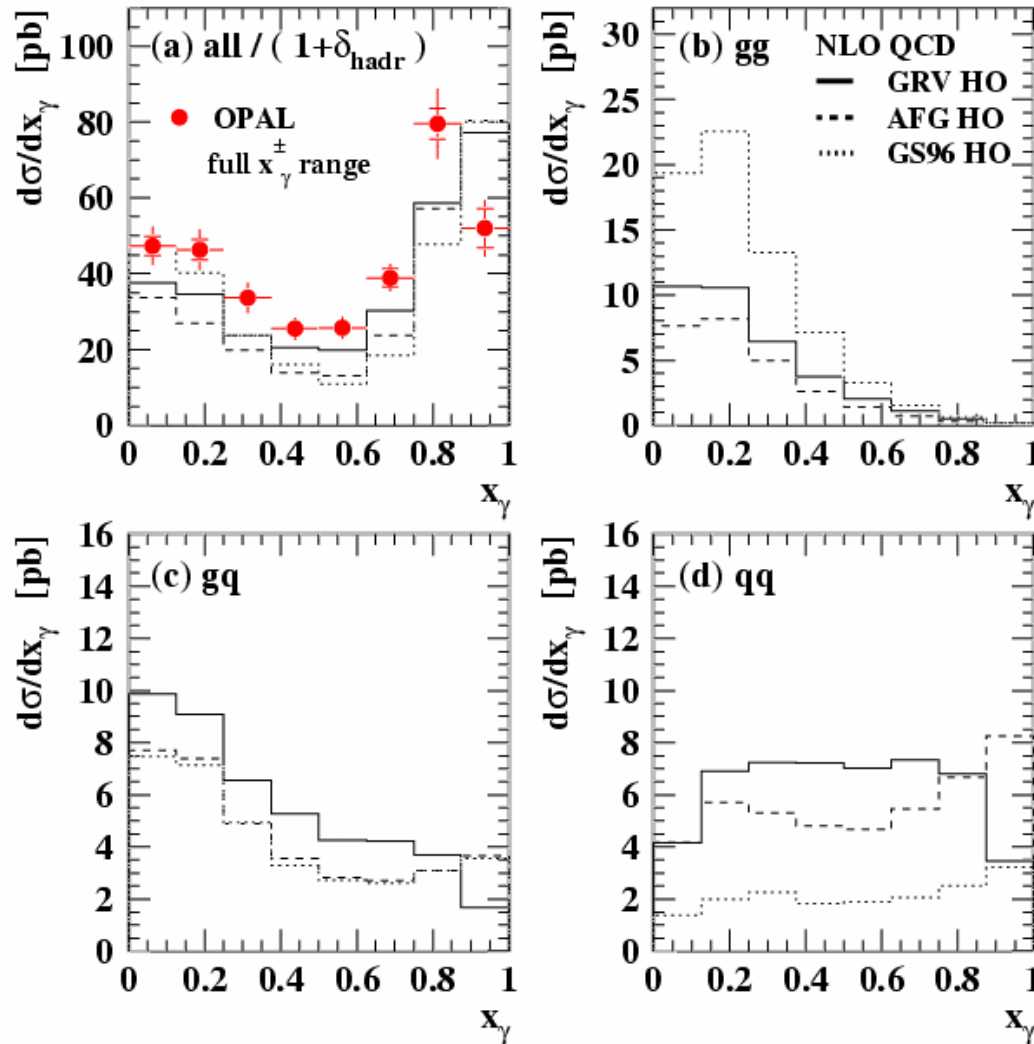
Example of hadronisation corrections (OPAL)



Large corrections at $x_\gamma \approx 1$
(better look at sum of the highest two bins in x_γ)

At high ET hadronisation corrections are small
 $\sim 5\text{-}10\%$

The influence of the choice of PDF on NLO (OPAL)

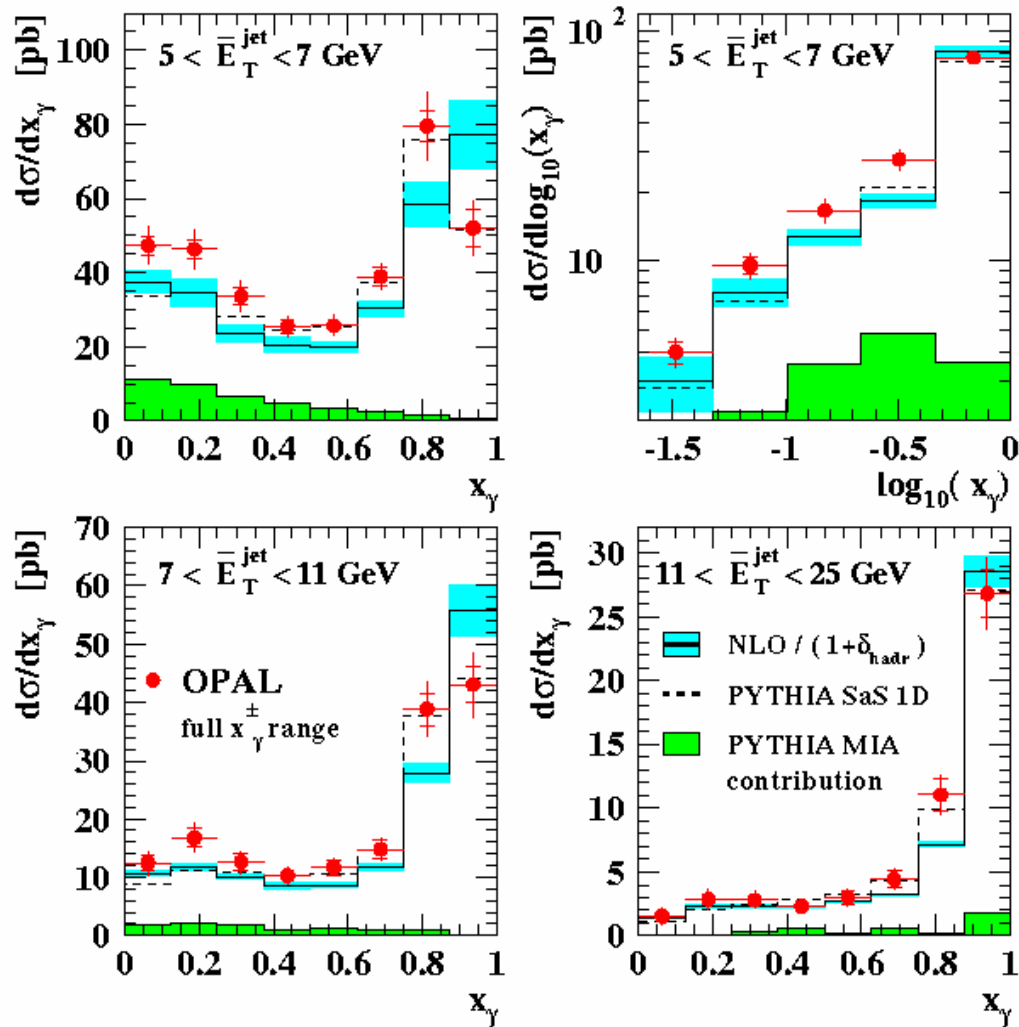


Gluonic processes are very sensitive to the amount of glue at low x_g

But for the cross-section this is compensated by inverse behavior of quark densities

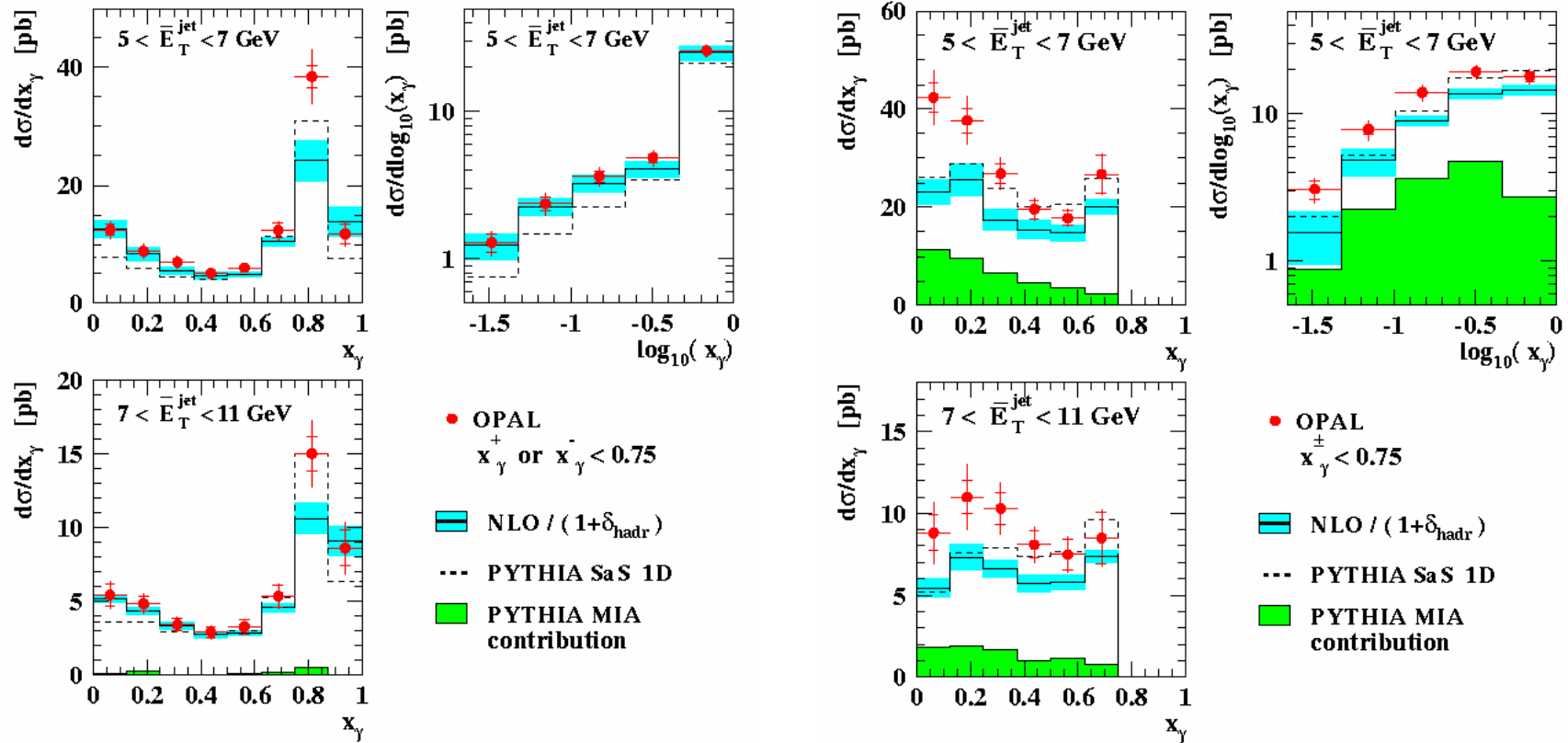
Need global fit to fix both at the same time ...

The di-jet cross-section vs. x_γ (OPAL)



Measurement for the full $x_\gamma^- - x_\gamma^+$ - space

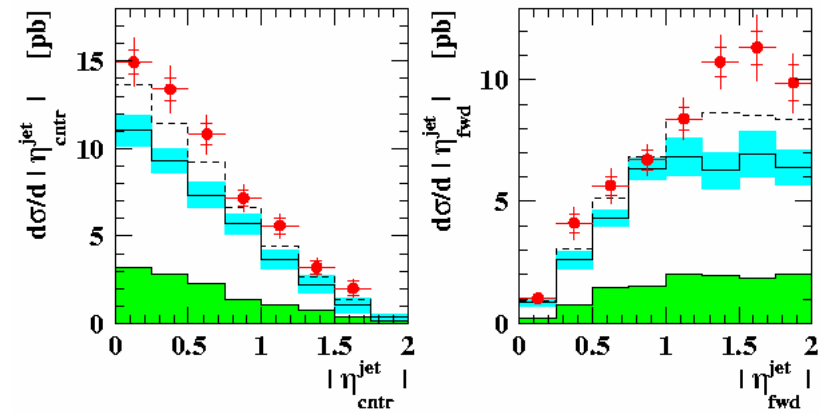
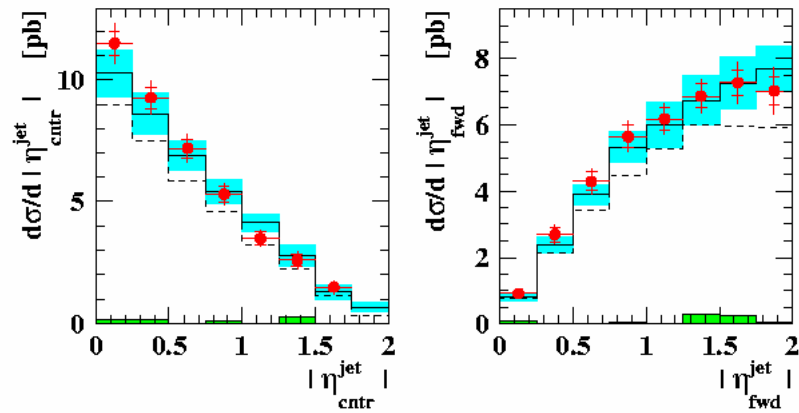
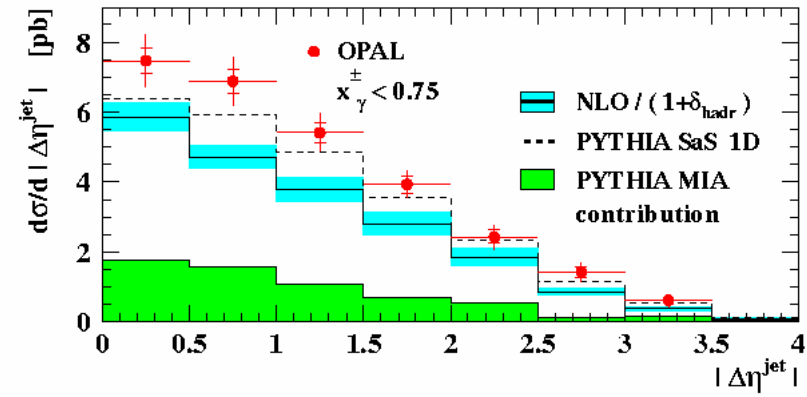
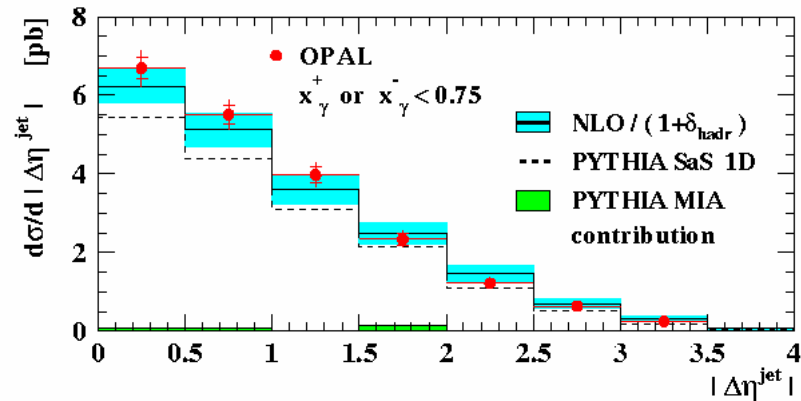
The di-jet cross-section vs. x_γ (OPAL)



“Single resolved enhanced”

“Double resolved enhanced”

The di-jet cross-section vs. η^{jet} (OPAL)



"Single resolved enhanced"

"Double resolved enhanced"

Di-jet x-section observables (OPAL)

$$\frac{d\sigma_{\text{dijet}}}{d\bar{E}_T^{\text{jet}}}$$

with $\bar{E}_T^{\text{jet}} \equiv \frac{E_{T,1}^{\text{jet}} + E_{T,2}^{\text{jet}}}{2}$ and $\bar{E}_T^{\text{jet}} > 5 \text{ GeV}$

$$\frac{d\sigma_{\text{dijet}}}{dx_\gamma}$$

in 3 bins of \bar{E}_T^{jet} [5 – 7 – 11 – 25] GeV

$$\frac{d\sigma_{\text{dijet}}}{d\log_{10}(x_\gamma)}$$

for $5 \text{ GeV} < \bar{E}_T^{\text{jet}} < 7 \text{ GeV}$

$$\frac{d\sigma_{\text{dijet}}}{d|\eta_{\text{cntr}}^{\text{jet}}|}, \frac{d\sigma_{\text{dijet}}}{d|\eta_{\text{fwd}}^{\text{jet}}|}, \frac{d\sigma_{\text{dijet}}}{d|\Delta\eta^{\text{jet}}|}$$

for $\bar{E}_T^{\text{jet}} > 5 \text{ GeV}$

$$\frac{d\sigma_{\text{dijet}}}{d|\cos\Theta^*|}$$

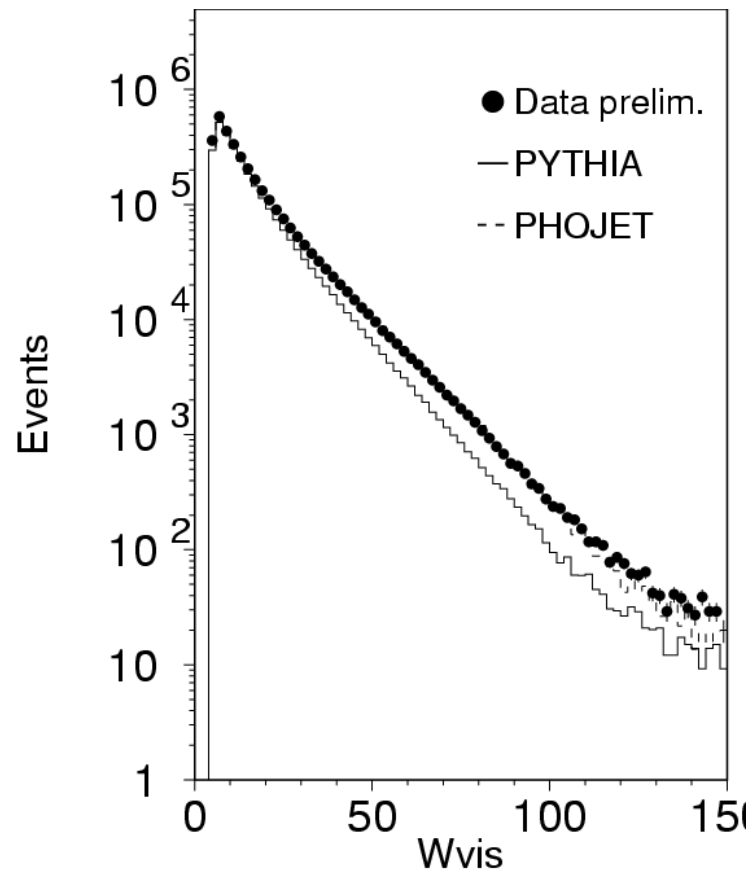
for $\bar{E}_T^{\text{jet}} > 5 \text{ GeV}$, $|\bar{\eta}^{\text{jet}}| < 1$, $M_{\text{jj}} > 15 \text{ GeV}$

with in all cases

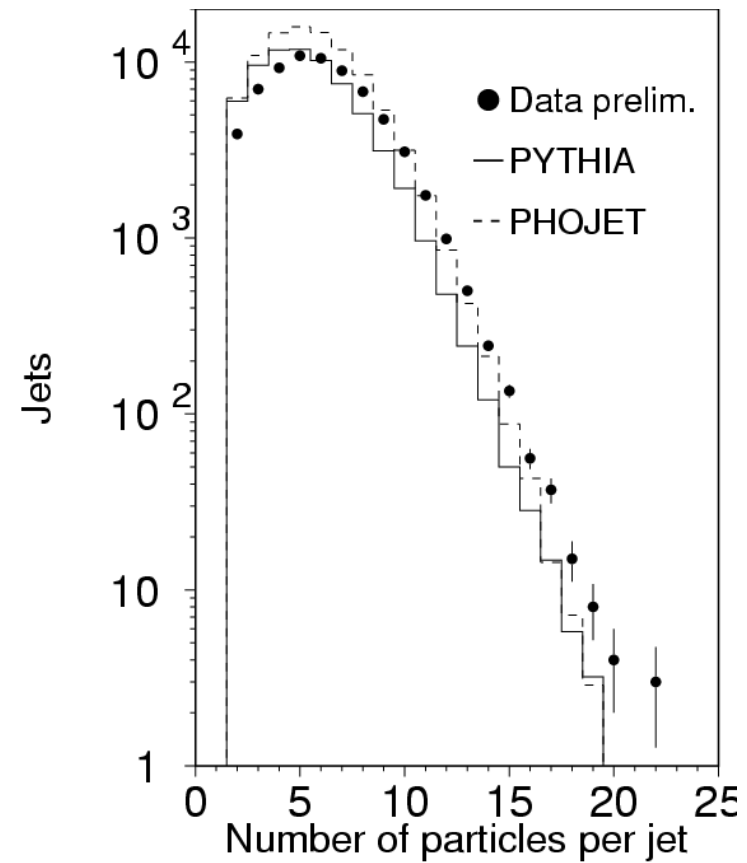
$$|\eta_{1,2}^{\text{jet}}| < 2 \quad \text{and} \quad \frac{|E_{T,1}^{\text{jet}} - E_{T,2}^{\text{jet}}|}{E_{T,1}^{\text{jet}} + E_{T,2}^{\text{jet}}} < \frac{1}{4}$$

Data / MC comparisons (L3 single jet analysis)

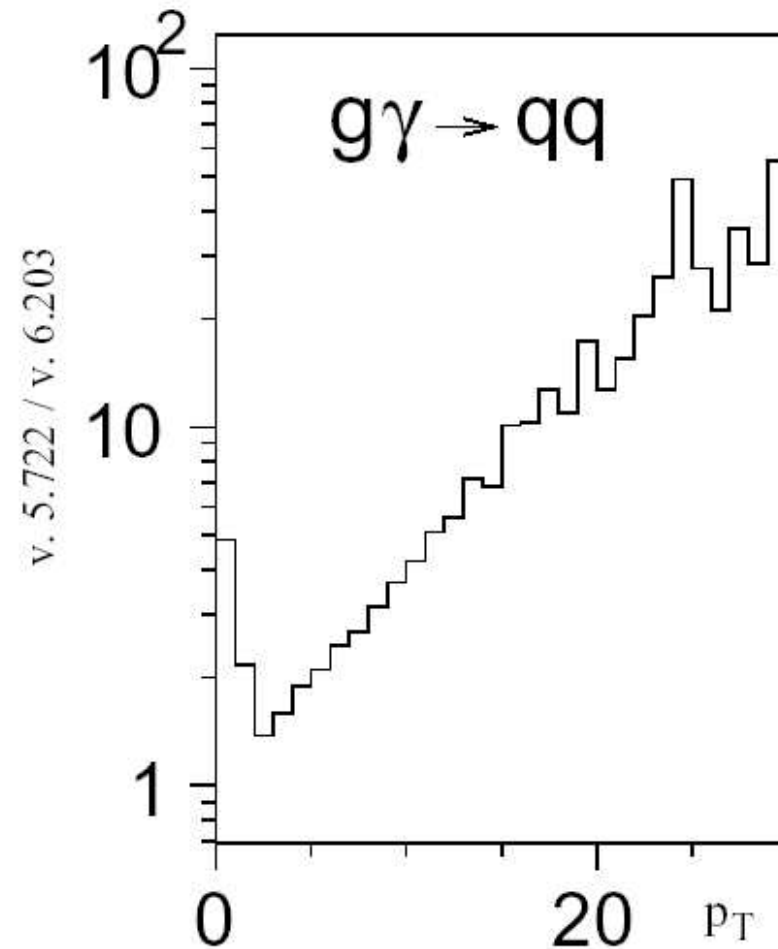
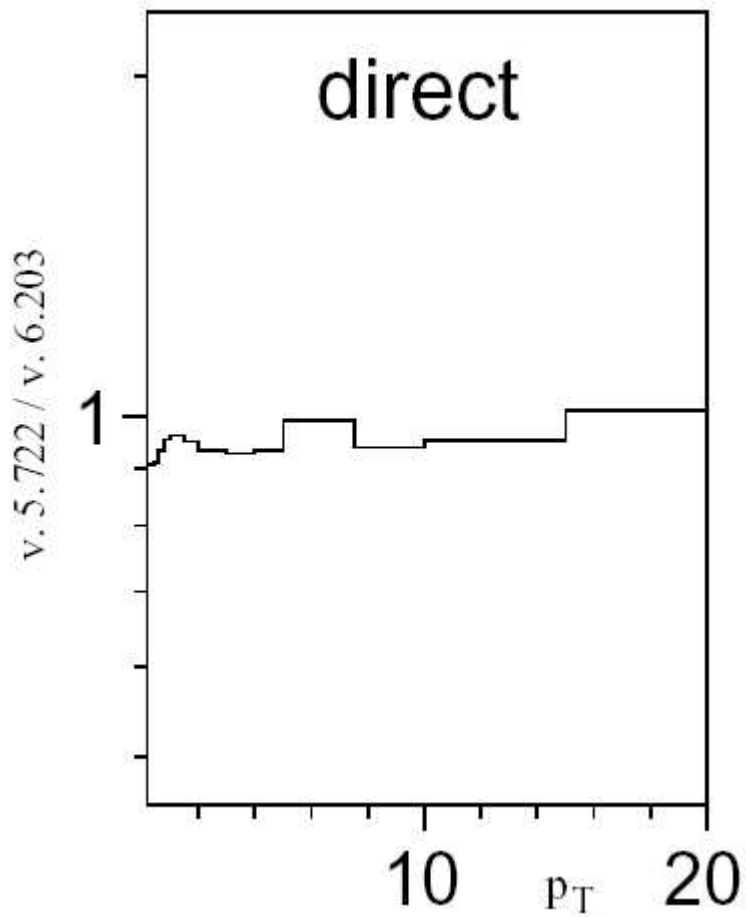
Invariant hadronic mass
after event selection



Number of particles per jet

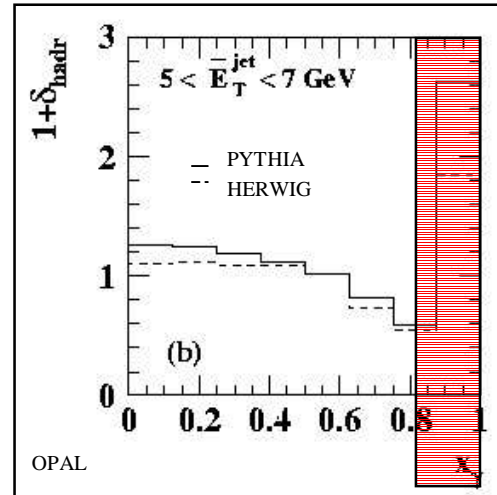
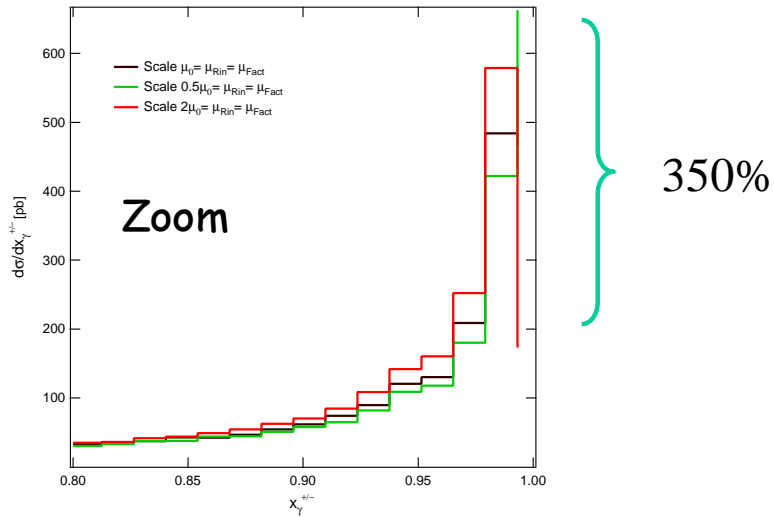


Changes in Pythia (hadron spectra, L3 study)



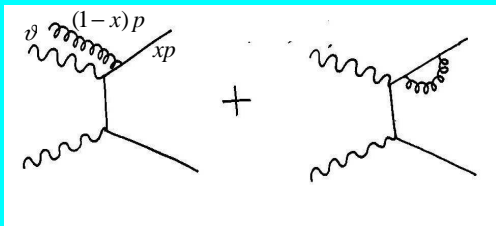
Dangerous regions:

$$1 + \delta_{hadr} = \frac{\sigma(\text{At the end of the "parton" shower})}{\sigma(\text{At the end of the hadronisation process})}$$



Failure of the perturbative computation

Recall our simple model to deal with the final state direct contribution in the dangerous region



$$\vartheta \rightarrow 0 \Rightarrow x \approx x_\gamma$$

$$x \rightarrow 1$$

$$\langle F \rangle_{NLO}^{Sub} \approx \int_0^1 dx \frac{F(x) - F(1)}{(1-x)} \quad \frac{d\sigma}{dx_\gamma} \Leftrightarrow F(x) = \delta(1-x_\gamma)$$

$$\frac{d\sigma}{dx_\gamma} \approx \left(\frac{1}{(1-x_\gamma)} - \frac{\theta(x_\gamma - 1)}{(1-x_\gamma)} \right) + \dots$$